Reheating after Gauss-Bonnet inflation

Bum-Hoon Lee[1,*] and Gansukh Tumurtushaa[2,†]

[1]*Department of Physics, Sogang University, Seoul 121-742, Korea,*
Center for Quantum Spacetime, Sogang University, Seoul 121-742, Korea
[2]*Center for Theoretical Physics of the Universe,*
Institute for Basic Science (IBS), Daejeon 34051, Korea

The physics of reheating after cosmic inflation is highly uncertain and unconstrained hence it is strongly model dependent. However, the duration of reheating and thermalization temperature at the end of reheating can be determined in terms of the equation-of-state parameter. By considering the chaotic inflation with the monomial coupling, we attempt to determine the equation-of-state parameter during reheating. Our result shows that $\omega_{\rm th} > 1/3$ is preferred in order for successful inflation to occur. Moreover, reheating lasts longer in our model and predicted reheating temperature at the end of reheating is lower than the standard scenario.

PACS numbers: 95.35.+d

I. INTRODUCTION

Inflationary scenario, in which the universe is assumed to be expanded quasi-exponentially, plays an important role in explaining the cosmological problems, including the flatness and the horizon problem, and providing a theory of the primordial spectrum of cosmological perturbation [1–4]. After inflation came to the end, the inflaton field is considered to be oscillating around the minimum of its potential hence it transfers its energy to the plasma of standard model particles. This period is known as the reheating.

The reheating phase can be characterized by three key parameters including the number $N_{\rm th}$ of e-folds, temperature $T_{\rm th}$ of reheating, and the equation-of-state $\omega_{\rm th}$ parameters [5]. These parameters can be linked to observable quantities of inflation such as the scalar and tensor spectral index, n_s and n_t, their running, α_s and α_t, tensor-to-scalar ration r, and the number of e-folds N_* during inflation [6–8].

Following the approach proposed in Refs. [6–8], in this paper we study several models of inflation with a Gauss-Bonnet term using $N_{\rm th}-n_s$ and $T_{\rm th}-n_s$ plane. Inflationary models with a Gauss-Bonnet term is not uncommon and has been well studied in inflation [11–14] as well as the physics of reheating [15, 16]. The inflation models with a Gauss-Bonnet term we have additional model parameters. Thus, we provide the constraints on model parameter in light of current and the accuracy of the future observation [2–4, 9, 10].

II. SETUP FOR GAUSS-BONNET INFLATION

The action we consider involves the Einstein-Hilbert term and the Gauss-Bonnet term that coupled with a canonical scalar field through coupling function $\xi(\phi)$,

$$S = \int d^4x\sqrt{-g}\left[\frac{R}{2\kappa^2} - \frac{1}{2}\partial_\mu\phi\partial^\mu\phi - V(\phi) - \frac{1}{2}\xi(\phi)R^2_{\rm GB}\right], \tag{1}$$

where $R^2_{\rm GB} = R_{\mu\nu\rho\sigma}R^{\mu\nu\rho\sigma} - 4R_{\mu\nu}R^{\mu\nu} + R^2$ is the Gauss-Bonnet term and $\kappa^2 = 8\pi G = M_{\rm pl}^{-2}$ is the reduced Planck mass. The Gauss-Bonnet coupling $\xi(\phi)$ is required to be a function of a scalar field in order to give nontrivial effects on the background dynamics. In a Friedmann-Robertson-Walker(FRW) universe with a scale factor a and a constant curvature K,

$$ds^2 = -dt^2 + a^2\left(\frac{dr^2}{1-Kr^2} + r^2d\Omega^2\right), \tag{2}$$

the background dynamics of this system yields the Einstein and the field equations

$$H^2 = \tfrac{\kappa^2}{3}\left[\tfrac{1}{2}\dot\phi^2 + V - \tfrac{3K}{\kappa^2a^2} + 12\dot\xi H\left(H^2 + \tfrac{K}{a^2}\right)\right], \tag{3}$$

$$\dot H = -\tfrac{\kappa^2}{2}\left[\dot\phi^2 - \tfrac{2K}{\kappa^2a^2} - 4\ddot\xi\left(H^2 + \tfrac{K}{a^2}\right) - 4\dot\xi H\left(2\dot H - H^2 - \tfrac{3K}{a^2}\right)\right], \tag{4}$$

$$0 = \ddot\phi + 3H\dot\phi + V_\phi + 12\xi_\phi\left(H^2 + \tfrac{K}{a^2}\right)\left(\dot H + H^2\right), \tag{5}$$

where a dot represents a derivative with respect to the cosmic time t, $H \equiv \dot a/a$ denotes the Hubble parameter, $V_\phi = \partial V/\partial\phi$, $\xi_\phi = \partial\xi/\partial\phi$, and $\dot\xi$ implies $\dot\xi = \xi_\phi\dot\phi$. Throughout this paper we consider the flat FRW universe with $K = 0$ for simplicity.

Although, similar works have been done in previous studies [15, 16], the aim of this work is to consider models which have not been previously studied and to provide the tight constraints on the range of model parameter. The model of interest in this work was, however, considered in Ref. [13] in a context of inflation.

*Electronic address: bhl@sogang.ac.kr
†Electronic address: gansuhmgl@ibs.re.kr

III. REHEATING PARAMETERS IN GAUSS-BONNET INFLATION.

Reheating is a transition era between the end of inflation and the beginning of the radiation-dominated era during which the energy stored in the scalarflied is converted to a plasma of relativistic particles. There is no direct cosmological observation are traceable this period of reheating hence the physics of reheating is highly uncertain and unconstrained. Thus the reheating is very model dependent. In this section, following the method proposed in Refs. [6–8], we derive analytic expressions for the reheating parameters for the Gauss-Bonnet inflation [13, 14] whereas next section is devoted to the numerical analysis of the current section.

Depending upon a model, reheating phase can be characterized by the effective equation-of-state parameter $\omega_{\rm th}$, which is defined by the effective pressure-to-energy-density ratio, the number of e-folds $N_{\rm th}$, which is considered as duration of reheating starting from the end of inflation until the beginning of radiation dominance, and the thermalization temperature $T_{\rm th}$ at the end of reheating phase. The value of $\omega_{\rm th}$ should be larger than $-1/3$ because inflation comes to an end when $\omega_{\rm th} = -1/3$ and is assumed to be smaller than 1 in order not to violate causality [**?**]. It is possible to achieve $\omega_{\rm th} \sim 1$ when potential energy dominates. For this reason, we will consider a broader range of $\omega_{\rm th} \in [-1/3, 1]$ in our numerical analysis.

Let us consider a mode with comoving wavenumber k_* which crosses the horizon during inflation when the scale factor is a_*. The comoving Hubble scale $a_* H_* = k_*$ at the horizon crossing time can be related to that of the present time as

$$\frac{k_*}{a_0 H_0} = \frac{a_*}{a_{\rm end}} \frac{a_{\rm end}}{a_{\rm th}} \frac{a_{\rm th}}{a_0} \frac{H_*}{H_0}\,, \tag{6}$$

where a_0, a_*, $a_{\rm end}$, and $a_{\rm th}$ denote the scale factor at present, the horizon crossing, the end of inflation, and the end of reheating, respectively. By taking logarithm from both sides, we rewrite Eq. (6) as

$$\ln \frac{k_*}{a_0 H_0} = -N_* - N_{\rm th} + \ln \frac{a_{\rm th}}{a_0} + \ln \frac{H_*}{H_0}\,, \tag{7}$$

where $N_* \equiv \ln(a_{\rm end}/a_*)$ is the number of e-foldings between the time of mode exits the horizon and the end of inflation, and $N_{\rm th} \equiv \ln(a_{\rm th}/a_{\rm end})$ is the number of e-foldings between the end of inflation and the end of reheating.

Following the standard assumption that entropy is preserved [6–8], no immense entropy production takes place after the end of reheating, we obtain the argument of the third term on rhs in Eq. (7) as,

$$\frac{a_{\rm th}}{a_0} = \frac{T_0}{T_{\rm th}} \left(\frac{43}{11 g_{\rm s,th}}\right)^{\frac{1}{3}}\,, \tag{8}$$

where $g_{\rm s,th}$ is the effective number of light species for entropy at the end of reheating. The reheating temperature $T_{\rm th}$ determines the energy density $\rho_{\rm th}$ at the end of reheating,

$$\rho_{\rm th} = \frac{\pi^2}{30} g_{\rm th} T_{\rm th}^4\,, \tag{9}$$

where $g_{\rm th}$ is the number of relativistic degrees of freedom in the end of reheating. On the other hand, the energy density $\rho_{\rm end}$ at the end of inflation is related to the energy density $\rho_{\rm th}$ at the end of reheating by $\omega_{\rm th}$ the equation-of-state parameter during reheating [6–8],

$$\rho_{\rm th} = \rho_{\rm end} e^{-3(1+\omega_{\rm th})N_{\rm th}}\,, \tag{10}$$

where it is worth to note that the energy density at the end of inflation is a model dependent parameter. Thus, for the Gauss-Bonnet inflation, we find the energy density at the end of inflation from Eq. (3) as

$$\rho_{\rm end} = \lambda_{\rm end} V_{\rm end}\,, \tag{11}$$

where $\lambda_{\rm end}$ is obtained[1] as

$$\lambda_{\rm end} = \frac{6}{6 - 2\epsilon - \delta_1(5 - 2\epsilon + \delta_2)}\,. \tag{12}$$

The slow-roll parameters ϵ, δ_1, and δ_2 are defined in terms of the inflaton potential and the GB coupling function as [13, 14]

$$\epsilon = \frac{1}{2\kappa^2}\frac{V_\phi}{V} Q\,, \tag{13}$$

$$\delta_1 = -\frac{4\kappa^2}{3}\xi_\phi V Q, \tag{14}$$

$$\delta_2 = -\frac{1}{\kappa^2}\left(\frac{\xi_{\phi\phi}}{\xi_\phi} Q + \frac{1}{2}\frac{V_\phi}{V} Q + Q_\phi\right)\,, \tag{15}$$

with

$$Q \equiv \frac{V_\phi}{V} + \frac{4}{3}\kappa^4 \xi_\phi V\,. \tag{16}$$

After substituting Eqs. (9)–(11) into Eq. (8), then into Eq. (7) we obtain

$$N_{\rm th} = \frac{4}{1 - 3\omega_{\rm th}}\left[60 - N_* - \ln\left(\frac{3\lambda_{\rm end}}{10\pi^2}\right)^{\frac{1}{4}} - \ln\left(\frac{V_{\rm end}^{\frac{1}{4}}}{H_*}\right)\right]\,, \tag{17}$$

where we used following numerical values $a_0 = 1$, $M_{\rm pl} = \kappa^{-1} = 2.435\times10^{18}$GeV, $T_0 = 2.725$K, 1Mpc $= 3.0857\times10^{24}$cm, 1K $= (0.23{\rm cm})^{-1}$, $g_{\rm th} = g_{\rm s,th} \simeq 10^3$, and $k = 0.05\,{\rm Mpc}^{-1}$ [3, 4]. Here, in above equation, the last three terms depend on inflationary models. Therefore, we will consider specific configuration of inflaton potential and coupling functions in next section. From Eqs. (9)–(10), it is straightforward to obtain the reheating temperature,

$$T_{\rm th} = \left(\frac{30\lambda_{\rm end} V_{\rm end}}{\pi^2 g_{\rm th}}\right)^{\frac{1}{4}} e^{-\frac{3}{4}(1+\omega_{\rm th})N_{\rm th}}\,. \tag{18}$$

---

[1] Eq. (11) is the model independent result while Eq. (12) is obtained only for our model in Eq. (1).

For the inflationary models with a Gauss-Bonnet term [13, 14], the number of e-folds from the moment the mode k_* crosses the horizon until the end of inflation is given by

$$N_* = \int_{t_*}^{t_{\rm end}} H dt \simeq \int_{\phi_{\rm end}}^{\phi_*} \frac{\kappa^2}{Q} d\phi, \tag{19}$$

where Q is given in Eq. (16). Using slow-roll approximation during inflation, we compute H_* from Eq. (3) as,

$$H_*^2 \simeq \frac{\kappa^2}{3} V(\phi_*)\,. \tag{20}$$

The next section is devoted to compute as well as to provide analysis on Eqs. (17)–(18) for the specific configurations of the potential and the Gauss-Bonnet coupling function.

IV. CHAOTIC INFLATION WITH THE MONOMIAL COUPLING

We will consider chaotic inflation with the monomial coupling given by

$$V(\phi) = \frac{V_0}{\kappa^4}(\kappa\phi)^n\,, \quad \xi(\phi) = \xi_0(\kappa\phi)^n\,. \tag{21}$$

In order to compute Eqs. (17)–(18) for Eq. (21), we need to know the scalar-field value at the end of inflation, $\phi_{\rm end}$, because that determines $V_{\rm end}$ and $\lambda_{\rm end}$ at the end of inflation. It is assumed that the effect of Gauss-Bonnet term is negligible in the vicinity of the end of inflation because this term is considered as a small correction to the Ricci scalar and this is justified in FIG 1 [12]. In the vicinity of end of inflation,

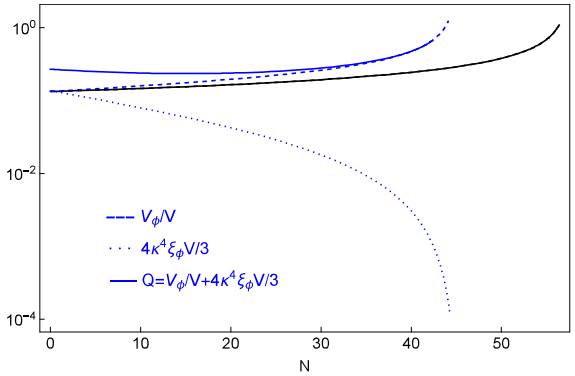

Figure 1: The evolution of Eq. (16) for the model Eq. (21) with $n = 2$. The potential parameter is set to $V_0 = 0.5\times10^{-12}$ while coupling parameter takes values including $\xi_0 = 0$(black) and $\xi = 3\times10^7$(blue). The labelling V_ϕ/V corresponds to the blue dashed line while $4\kappa^4\xi_\phi V/3$ labelling corresponds to the blue dotted line. The black and the blue solid lines correspond to labelling Q.

as the potential slope gets steeper, the first term in Eq. (16) grows while the second term decays, as seen in FIG. 1. Thus, one can approximate Eq. (16) at the end of inflation as

$$Q \simeq \frac{V_\phi}{V}\,. \tag{22}$$

By using Eq. (22), we rewrite Eqs. (13)–(15) at the end of inflation as

$$\epsilon \simeq \frac{1}{2\kappa^2}\left(\frac{V_\phi}{V}\right)^2, \tag{23}$$

$$\delta_1 \simeq -\frac{4\kappa^2}{3}\xi_\phi V_\phi, \tag{24}$$

$$\delta_2 \simeq -\frac{1}{\kappa^2}\left[\frac{\xi_{\phi\phi}}{\xi_\phi}\frac{V_\phi}{V} + \frac{V_{\phi\phi}}{V} - \frac{1}{2}\left(\frac{V_\phi}{V}\right)^2\right], \tag{25}$$

and these equations applicable only in the vicinity of the end of inflation. Thus these approximated equations are enough for our purpose. For the configurations given in Eq. (21), from Eqs. (23)–(25), we find

$$\epsilon = \frac{n^2}{2\kappa^2\phi^2},\ \delta_1 = -\alpha n^2(\kappa\phi)^{2n-2},\ \delta_2 = \frac{(4-3n)n}{2\kappa^2\phi^2}, \tag{26}$$

where $\alpha \equiv 4V_0\xi_0/3$. Inflation is assumed to come to the end when the first slow-roll parameter becomes order of unity, $\epsilon \equiv 1$. The field value at end of inflation can be obtained from first equation in Eq. (26) as $\phi_{\rm end}^2 = n^2/(2\kappa^2)$. The potential at the end of inflation, therefore, is

$$V_{\rm end} = \frac{V_0}{\kappa^4}\left(\frac{n^2}{2}\right)^{n/2}. \tag{27}$$

Eq. (26) also helps us to find $\lambda_{\rm end}$ value at the end of inflation as

$$\lambda_{\rm end} = \frac{3}{2}\left[1 - \frac{2\alpha}{n}\left(\frac{n^2}{2}\right)^n\right], \tag{28}$$

which is consistent with Ref. [6–8] in $\alpha \to 0$ limit. After substituting Eq. (21) into Eq. (19), we find

$$N_* = \frac{\kappa^2\phi_*^2}{2n}\,{}_2F_1\left(1, \frac{1}{n}; 1+\frac{1}{n}; -\alpha(\kappa\phi_*)^{2n}\right), \tag{29}$$

where ${}_2F_1$ is the hypergeometric function and the large-field inflation, $\phi_* \gg \phi_{\rm end}$, is assumed. When $n = 2$, Eq. (29) becomes

$$N_* = \frac{1}{4\sqrt{\alpha}}\arctan\left(\sqrt{\alpha}\kappa^2\phi_*^2\right), \tag{30}$$

where and hereafter in this section we set $n = 2$ for simplicity. Hubble parameter at the time of horizon crossing, therefore, is obtained from Eq. (20) as,

$$H_* = \sqrt{\frac{V_0}{3\kappa^2}}\left(\frac{1}{\sqrt{\alpha}}\tan\left(4\sqrt{\alpha}N_*\right)\right)^{\frac{1}{2}}. \tag{31}$$

We obtain the observable quantities such as the scalar spectral index n_s and tensor-to-scalar ration r in terms of N_* in our previous work [13],

$$n_s - 1 \simeq -\frac{2}{N_*} + 32\alpha N_*\,, \tag{32}$$

$$r \simeq \frac{8}{N_*} + \frac{640}{3}\alpha N_*\,. \tag{33}$$

From Eq. (32), we find

$$N_* = \frac{(n_s - 1) + \sqrt{(n_s - 1)^2 + 256\alpha}}{64\alpha}\,, \qquad (34)$$

and then Eq. (31) becomes

$$H_* = \sqrt{\frac{V_0}{3\kappa^2}}\left[\frac{1}{\sqrt{\alpha}}\tan\left(\frac{(n_s-1)+\sqrt{(n_s-1)^2+256\alpha}}{16\sqrt{\alpha}}\right)\right]^{\frac{1}{2}}. \qquad (35)$$

After substituting Eq. (27), Eq. (28), Eq. (34), and Eq. (35) into Eqs. (17)–(18), we obtain the number of e-folding $N_{\rm th}$, as well as the temperature of reheating $T_{\rm th}$. In FIG. 2, we plot Eqs. (17)–(18) for $\omega_{\rm th} = -1/3, 0, 1/6, 2/3$; solid, dashed, dot-dashed, and dotted respectively. If the reheating instantaneously occured right after the end of inflation, in which $N_{\rm th} = 0$, the energy density stored in the inflaton field must have converted into the radiation energy density instantaneously. Thus, the instantaneous reheating temperature peaks at $T_{\rm th} = 6.3274 \times 10^{14}$ GeV, regardless of the value of the model parameter α. However, the spectral index value is fixed at $n_s = 0.9644$ for the standard slow-roll inflation case (the black point in the middle panel). For the positive values of α are allowed, in which the n_s value shifts to the left (to the smaller n_s value). In plotting red curves in FIG. 2, *for example*, we set $\alpha = 6.032 \times 10^{-7}$, and all curves intersect at $n_s = 0.963$ (the red points) indicating the instantaneous reheating. The positive values of α between $2.1283 \times 10^{-8} \leq \alpha \leq 1.019 \times 10^{-6}$ stay inside the 1σ contour of the current observation and the corresponding range of n_s is between $0.962 \leq n_s \leq 0.9644$.

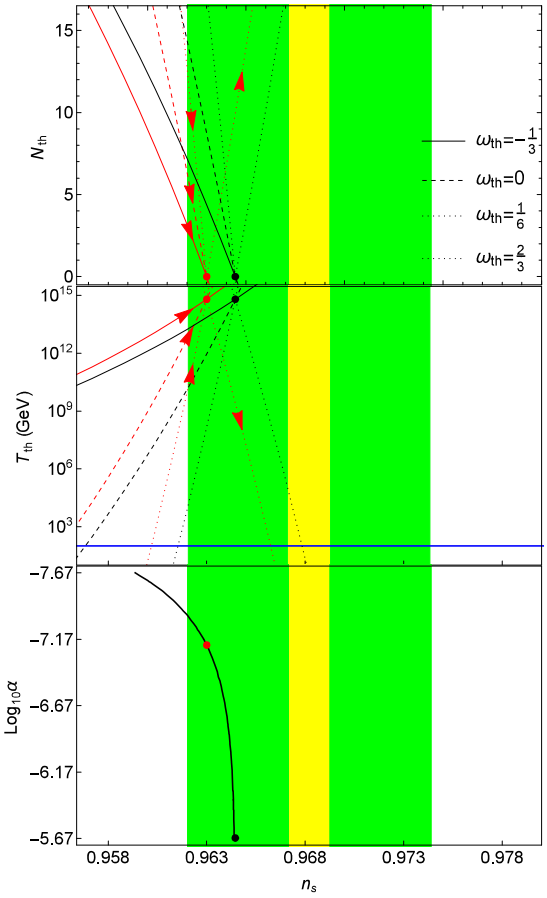

Figure 2: (Color online) Plots of the duration $N_{\rm th}$ and the temperature $T_{\rm th}$ of the reheating for Eq. (21). For the black curves, the GB term is absent ($\alpha = 0$), and it is present with $\alpha = 6.032 \times 10^{-7}$ for red ones. The bottom panel shows the curve of the instantaneous reheating where $N_{\rm th} = 0$. The green shaded region shows the current 1σ bounds on n_s from Planck data while the yellow one indicates the 1σ bounds of future CMB experiments with sensitivity $\pm 10^{-3}$ [9, 10], using the same central n_s value as Planck. The blue horizontal line at 100GeV corresponds to the electro-weak energy scale. The arrows indicate that N_* increases along the curve, same behavior applies for the black curves as well.

In case the reheating epoch lasted for certain number $N_{\rm th} \neq 0$ of e-folds, one can see from FIG. 2 that the duration of reheating is shorter in our model with the GB term (the red curves) than the standard scenario (the black curves), but this is true only for $\omega_{\rm th} < 1/3$. Contrary, the reheating is longer in the red curves than the black ones if $\omega_{\rm th} > 1/3$. If the duration of reheating is shorter for the models with the GB term, then the temperature at the end of reheating is higher than the standard case, and vise versa.

Furthermore, for the model, which is given in Eq. (21), the theoretical predictions tend to stay outside the 2σ contour of the Planck 2015 data when $N_* < 60$ values because of their prediction of the large tensor-to-scalar ration. Since $N_* \geq 60$ is favored by the data, the preferred value of the equation-of-state parameter must be $\omega_{\rm th} > 1/3$ for our model in Eq. (21). Moreover, due to the presence of the GB term, the duration of reheating is longer in the model than the standard scenario, and the predicted reheating temperature is lower than the standard case.

V. CONCLUSION

We considered Gauss-Bonnet inflation to obtain the key parameters during reheating. Our analytic results are obtained in Sec. III where we computed the duration and the temperature at the end of reheating in terms of the effective equation-of-state parameter. Since the physics of reheating epoch is highly model dependent, we specified our model to be the chaotic inflation with the monomial coupling to Gauss-Bonnet term, as given in Eq. (21). After deriving the necessary quantities for our model, we investigated numerical analysis in Sec.IV.

As a result we showed that $\omega_{\rm th} > 1/3$ is favored by the observational Planck data. Moreover, reheating lasts longer in our model and predicted reheating temperature at the end of reheating is lower than the standard scenario.

In this work, for simplicity, we adopted two as-

sumptions. First, we assumed the equation-of-state parameter to be constant throughout the reheating era. Second assumption that we accepted is that the entropy is preserved after the completion of reheating. Although these assumptions are acceptable, one can consider further extensions of these assumptions. For instance, one can do the same analysis by considering both the varying equation-of-state parameter and the other processes such as another scalar-field dominated era after the reheating. We leave them as our future work and the further continuation of the current work.

Acknowledgments

Authors thank to Prof. Seoktae Koh from Jeju National University for useful discussions and valuable comments. The work of G. T was supported by IBS under the project code, IBS-R018-D1.

[1] A. H. Guth, "The Inflationary Universe: A Possible Solution to the Horizon and Flatness Problems," Phys. Rev. D **23**, 347 (1981).

[2] G. Hinshaw *et al.* [WMAP Collaboration], "Nine-Year Wilkinson Microwave Anisotropy Probe (WMAP) Observations: Cosmological Parameter Results," Astrophys. J. Suppl. **208**, 19 (2013);
E. Komatsu *et al.* [WMAP Collaboration], "Seven-Year Wilkinson Microwave Anisotropy Probe (WMAP) Observations: Cosmological Interpretation," Astrophys. J. Suppl. **192**, 18 (2011);
E. Komatsu *et al.* [WMAP Collaboration], "Five-Year Wilkinson Microwave Anisotropy Probe (WMAP) Observations: Cosmological Interpretation," Astrophys. J. Suppl. **180**, 330 (2009);

[3] P. A. R. Ade *et al.* [Planck Collaboration], "Planck 2013 results. XXII. Constraints on inflation," Astron. Astrophys. **571**, A22 (2014);

[4] P. A. R. Ade *et al.* [Planck Collaboration], "Planck 2015 results. XX. Constraints on inflation," arXiv:1502.02114 [astro-ph.CO].
A. Albrecht and P. J. Steinhardt, "Cosmology for Grand Unified Theories with Radiatively Induced Symmetry Breaking," Phys. Rev. Lett. **48**, 1220 (1982).
A. D. Linde, "A New Inflationary Universe Scenario: A Possible Solution of the Horizon, Flatness, Homogeneity, Isotropy and Primordial Monopole Problems," Phys. Lett. B **108**, 389 (1982).

[5] R. G. Cai, Z. K. Guo and S. J. Wang, "Reheating phase diagram for single-field slow-roll inflationary models," Phys. Rev. D **92**, 063506 (2015)

[6] L. Dai, M. Kamionkowski and J. Wang, "Reheating constraints to inflationary models," Phys. Rev. Lett. **113**, 041302 (2014)

[7] P. Creminelli, D. Lpez Nacir, M. Simonovi?, G. Trevisan and M. Zaldarriaga, "ϕ^2 Inflation at its Endpoint," Phys. Rev. D **90**, no. 8, 083513 (2014)

[8] J. B. Munoz and M. Kamionkowski, "Equation-of-State Parameter for Reheating," Phys. Rev. D **91**, no. 4, 043521 (2015)

[9] L. Amendola *et al.* [Euclid Theory Working Group Collaboration], "Cosmology and fundamental physics with the Euclid satellite," Living Rev. Rel. **16**, 6 (2013)

[10] P. Andre *et al.* [PRISM Collaboration], "PRISM (Polarized Radiation Imaging and Spectroscopy Mission): A White Paper on the Ultimate Polarimetric Spectro-Imaging of the Microwave and Far-Infrared Sky,"

[11] Z. K. Guo and D. J. Schwarz, "Slow-roll inflation with a Gauss-Bonnet correction," Phys. Rev. D **81**, 123520 (2010)

[12] M. Satoh, "Slow-roll Inflation with the Gauss-Bonnet and Chern-Simons Corrections," JCAP **1011** (2010) 024.

[13] S. Koh, B. H. Lee, W. Lee and G. Tumurtushaa, "Observational constraints on slow-roll inflation coupled to a Gauss-Bonnet term," Phys. Rev. D **90**, no. 6, 063527 (2014);

[14] S. Koh, B. H. Lee and G. Tumurtushaa, "Reconstruction of the Scalar Field Potential in Inflationary Models with a Gauss-Bonnet term," arXiv:1610.04360 [gr-qc].

[15] C. van de Bruck, K. Dimopoulos and C. Longden, "Reheating in Gauss-Bonnet-coupled inflation," Phys. Rev. D **94**, no. 2, 023506 (2016)

[16] S. Bhattacharjee, D. Maity and R. Mukherjee, "Constraining scalar-Gauss-Bonnet Inflation by Reheating, Unitarity and PLANCK," arXiv:1606.00698 [gr-qc].

Peculiarities of matrix-element calculations with few Coulomb functions for particles' scattering processes

O. Chuluunbaatar[1,2,*], K.A. Kouzakov[3], A.G. Galstyan[4], Yu.V. Popov[5,6], M.S. Schoffler[7]

[1]*LIT, Joint Institute for Nuclear Research, Dubna, Moscow region 141980, Russia*

[2]*Institute of Mathematics, National University of Mongolia, UlaanBaatar, Mongolia*

[3]*Department of Nuclear Physics and Quantum Theory of Collisions, Faculty of Physics, Lomonosov Moscow State University, Moscow 119991, Russia*

[4]*Institute of Condensed Matter and Nanosciences, Universit´e catholique de Louvain, B-1348 Louvain-la-Neuve, Belgium*

[5]*BLTP, Joint Institute for Nuclear Research, Dubna, Moscow region 141980, Russia*

[6]*Skobeltsyn Institute of Nuclear Physics, Lomonosov Moscow State University, Moscow 119991, Russia*

[7]*Institut f¨ur Kernphysik, Universit¨at Frankfurt, 60438 Frankfurt, Germany*

[*]Electronic address: chuka@jinr.ru

We present ultra high resolution data on single ionization of helium under impact of 1-MeV protons in comparison with theoretical calculations. Good agreement between theory and experiment [1] is obtained. Three initial trial helium wave functions are employed: a weakly correlated Roothaan-Hartree-Fock function, a simple Silverman-Platas-Matsen function of the configuration interaction family, and a strongly correlated function [2,3]. Multidimensional singular integrals which defining differential cross sections are calculated using special transform for each above trial function. Results of some calculations are presented in Figure 1.

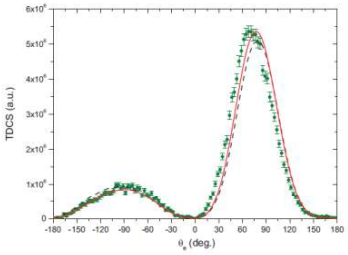

Fig.1. Triple Differential Cross Section in coplanar geometry versus the angle of escaped electron: Plane Wave First Born Approximation (black dashed line) and 3C final correlated wave function + highly correlated helium ground state [2] (red solid line). Experimental values [1] are represented by green points.

References

[1] O. Chuluunbaatar, S. A. Zaytsev, K. A. Kouzakov, A. Galstyan, V. L. Shablov, and Yu. V. Popov, Phys. Rev. A accepted (2017).

[2] H. Gassert, O. Chuluunbaatar et al., Phys. Rev. Lett. 116, 073201 (2016).

[3] O. Chuluunbaatar, I. V. Puzynin, P. S. Vinitsky, Yu. V. Popov, K. A. Kouzakov, and C. Dal Cappello, Phys. Rev. A 74, 014703 (2006).